Chapter 4: Graphitisation

4.1 Introduction

Graphitisation in the diamond-alumina interface was seen as a possible cause of lack of bonding. For this reason, special attention is given to this topic.

Literature on the graphitisation of diamond can be divided into four categories:

- Graphitisation of diamond by itself, i.e. not in contact with any matrix,
- Graphitisation in oxide ceramic matrices,
- Graphitisation in non-oxide ceramic matrices, and
- Graphitisation in metal matrices.

The distinction between oxide and non-oxide matrices is made, since the graphitisation in non-oxide matrices is not applicable to this work. Other oxide matrices might be expected to affect diamond in the same way as alumina due to the presence of an oxygen potential. Non-oxides, of course, do not have an oxygen potential. Non-oxide matrices were therefore not considered in this literature survey. Likewise, metal matrices were ignored.

Graphitisation depends on various factors, including diamond type, pressure, temperature, oxygen partial pressure (Liu and Ownby, 1991), the presence of other forms of chemical attack (Pipkin, personal communication) and even the way of heating (Sozin *et al*, 1992). Of these, the effects of temperature, pressure and oxygen pressure are of relevance in this work and are discussed here.

4.2 Graphitisation of non-integrated diamond

As the pressure-temperature diagram in fig. 4-1 shows, diamond is only metastable at pressures of less than 40 kbar (and below 4000 K), with graphite being the more stable phase. At low temperature the rate of conversion to graphite is, of course, utterly insignificant, as exemplified by very old deposits of natural diamond. At high temperature (> ~ 1 000 °C) the conversion to graphite accelerates significantly.

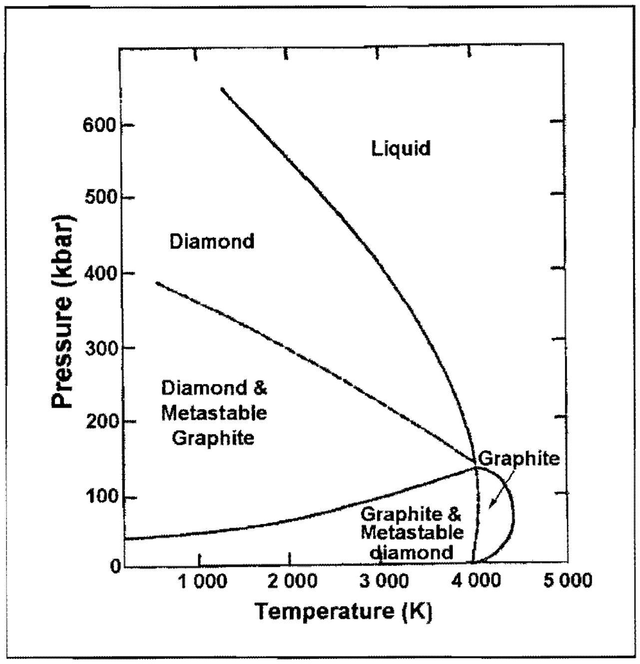

***Fig. 4-1**: Carbon phase diagram (Pierson, 1993). The entire diagram is included for interest; actually the only area of interest falls in the stable graphite area, at the lowest part of the diagram.*

The mechanism of graphitisation seems to be the detachment of singe carbon atoms from the diamond surface, followed by their condensation as graphite. This theory is supported by comparison between the activation energy of graphitisation and the vaporisation energy of diamond. Vaporisation entails detachment of single atoms, as opposed to groups of atoms. Since the activation energy of graphitisation is similar to that of vaporisation, it is likely that graphitisation also entails single atom detachment (Evans, 1979).

Any chemical attack on diamond might induce and accelerate graphitisation (Pipkin, personal communication). Graphitisation accompanies the oxidation of diamond surfaces and oxygen actually seems to catalyse thermal graphitisation (Evans and Phaal, 1962; Evans, 1994a, b). This has the result that the temperature at which graphitisation starts varies with the concentration of surrounding gaseous species. In fig. 4-2, several data of the extent of graphitisation at high temperature in the presence of oxygen or under vacuum are compared. If the general tendency of these data is followed, it seems as though the oxygen potential of alumina would start to cause graphitisation at around 1 700 °C. However the presence of titanium (from the HIPping capsules), as is the case in experimental work done for this thesis, would decrease the oxygen potential, as titanium is an reduction agent. The above deduction may therefore not be valid in the case of HIPping in the experiments of this work, since the possible influence of titanium is not investigated further.

Graphitisation starts at discrete sites on the surface and spreads out. After covering the surface, graphitisation proceeds into the diamond. Graphitisation is essentially a surface phenomenon, although limited graphitisation can occur internally (Evans, 1979, 1992; Noma and Sawaoka, 1985).

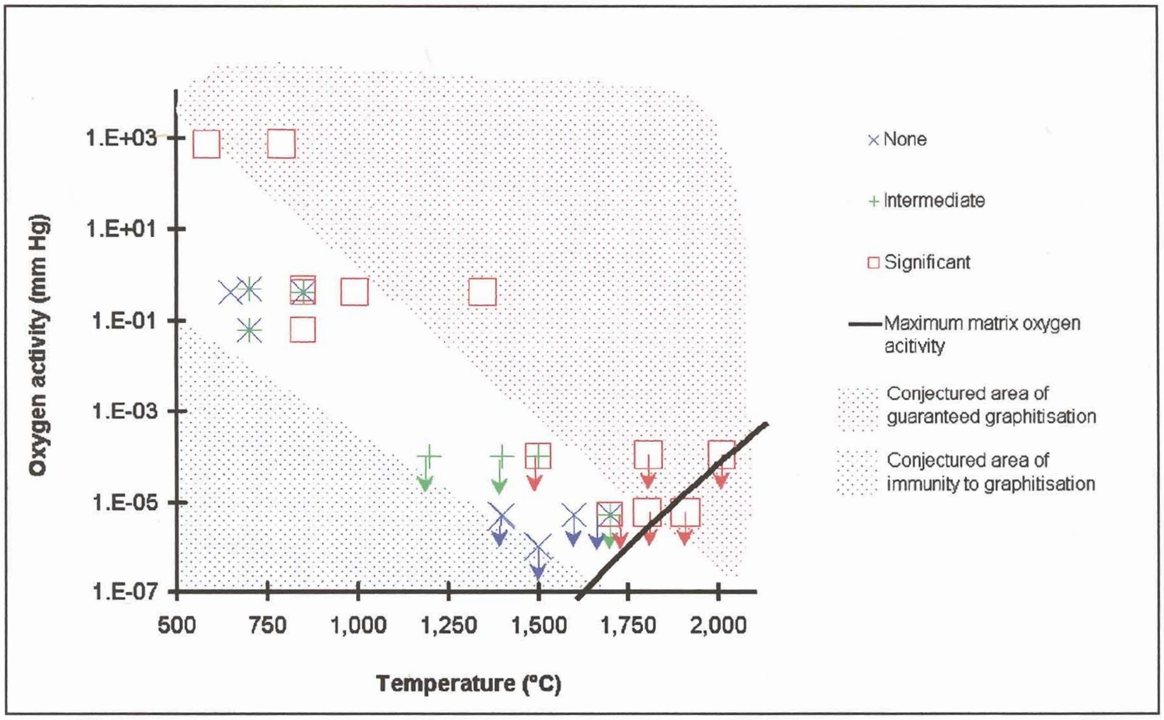

***Fig. 4-2**: Graphitisation as an effect of oxygen potential and temperature (Data from Howes, 1962; Seal, 1958; Evans and Phaal, 1962; and Liu and Ownby, 1991. See appendix A2 for details of the diagram's construction and its limitations.)*

The only work on the kinetics of graphitisation is that of Davies (1972) and Davies and Evans (1972). They proposed a first order equation that accounts for the dual effect of temperature and pressure:

$$\frac{\delta L_{\text{graphitisation}}}{\delta t} = k_{DE} e^{\frac{-E+PV}{RT}} \qquad (4\text{-}1)$$

The coefficient k_{DE} incorporates the effect of the number of graphitisation sites. If the diamond surface is not saturated with sufficient sites, or not adequately 'rough', k_{DE} is not constant initially. It is only constant after a graphite layer has spread over the surface and, consequently, the surface is saturated with graphitisation sites. No values for k_{DE} are given even though they can be calculated from the experimental data. Much uncertainty is involved with the coefficient k_{DE} and the primary aim of the work was to determine activation energy (Davies, personal communication). Nonetheless, some indication of the relative magnitude of the graphitisation rates on the three low index faces of diamond is given. The rate of graphitisation is very much dependent on the exposed face of the diamond and follows the trend: {110}>{111}>>{100}. In table 4-1, the rate of graphitisation on the {110} and {111} faces is compared at specific temperatures. Specific quantitative data are not available for oxygen catalysed graphitisation, but it is known that the {100} face is also more resistant in the presence of oxygen (Evans, 1979).

Arrhenius plots for the {110} and {111} faces (at zero pressure) are given in fig. 4-3 and 4-4, and values for the activation energy, $\mathcal{E}$ and activation volume $\mathcal{V}$ are given in table 4-2.

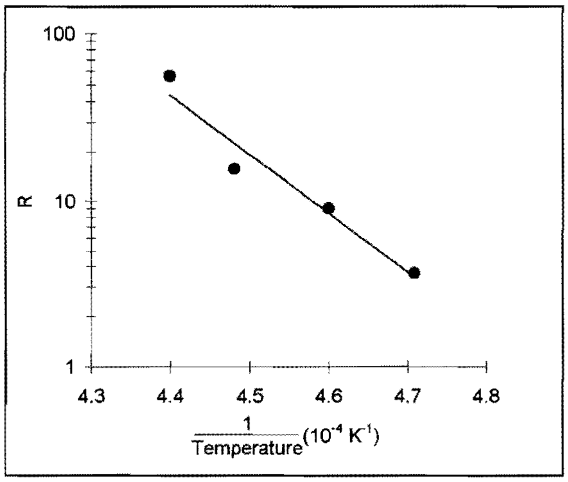

Fig. 4-3: *Arrhenius plot for the {110} face. R is directly proportional to the graphitisation rate. (Davies, 1972.)*

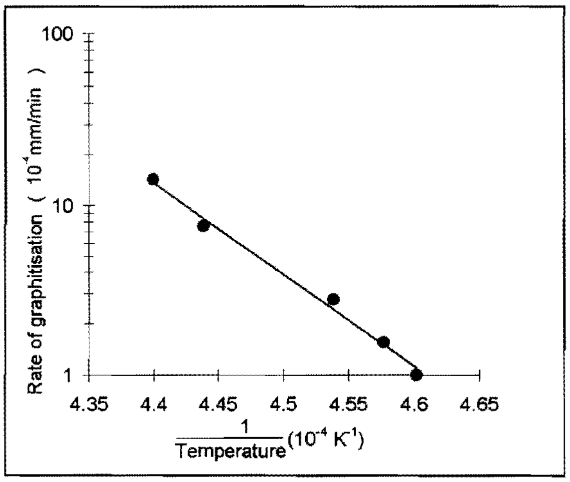

Fig. 4-4: *Arrhenius plot for the {111} face. (Davies, 1972.)*

Table 4-1: *Comparison of graphitisation rates on low index faces.*

Temperature (°C)	$\left(\frac{\delta L_{(110)}}{\delta t} \middle/ \frac{\delta L_{(111)}}{\delta t}\right)_{graphitisation}$
1 900	70
1 700	30

Table 4-2: *Activation energy and activation volumes for graphitisation*

Face	$\mathcal{E}$ (kJ/mol)	$\mathcal{V}$ (cm^3/mol)
{110}	730 ± 50	10.2 ± 3
{111}	1 060 ± 80	9.7 ± 2

4.3 Graphitisation of diamond in oxide matrices

Available data for graphitisation in alumina matrices are summarised in table 4-3, which compares the extent of graphitisation encountered by different authors.

***Table 4-3**: Graphitisation in alumina matrices*

Densification					Analysis		Reference
Method	Temperature (°C)	Solid pressure (kbar)	Duration (h)	Atmosphere	Method	Amount of graphitisation (%)	
Hot press	1 250	0.32	Not given	Ar	Powder XRD	0	Liu and Ownby (1991)
Degassing followed by	500		2	0.0008 mm Hg vacuum	XRD	15	Noma and Sawaoka (1984)
'high pressure sintering'	1 300	60	1				
Degassing followed by	500		1	0.0008 mm Hg vacuum	XRD?	15	Noma and Sawaoka (1985)
'high pressure sintering'	1 300	60	1				
HIP	1 200	1.5	3		Not given	0	Kume *et al* *(1992)*
Hot press	1 550	0.35	c. 0.25	1.5×10^{-5} mm Hg vacuum	XRD	0	Chu *et al* (1992)

The emphasis in this work has been the suppression of graphitisation to enhance alumina-diamond bonding. Noma and Sawaoka (1984, 1985) followed the approach of intentionally graphitising the diamond for the toughening effect of the volume expansion on graphitisation (0.28 cm^3/g to 0.44 cm^3/g). This graphitisation was done in addition to the graphitisation already existing after firing. It is interesting to note in fig. 4-5 that extensive graphitisation still occurred in a dense (> 99 % theoretical density) composite, even though one might assume that diamond particles, being restricted in rigid voids, do not graphitise readily. Details of the toughening effect of graphitisation are given in chapter 5. Noma and Sawaoka (1985) also reported a significant change in the aspect ratio of diamond particles accompanied by internal layered graphitisation after extended post-hot pressing heat treatment. This will weaken diamond particles, and limit the reinforcement provided to the matrix. Noma and Sawaoka do not explain the change in aspect ratio, but the difference in graphitisation rates depending on the specific crystallographic face (mentioned in section 4.2) suggests a possible mechanism.

4.4. Raman analysis

Raman analysis is a convenient tool for identifying graphitisation. It is a particularly useful as diamond exhibits a distinct peak as shown in fig 4-6. Diamond particles without graphitised surfaces would show up as distinct peaks, while other forms of carbon also show on a Raman spectrum. Spectra for other forms of carbon are shown in fig.'s 4-7 and 4-8. In fig. 4-9 the

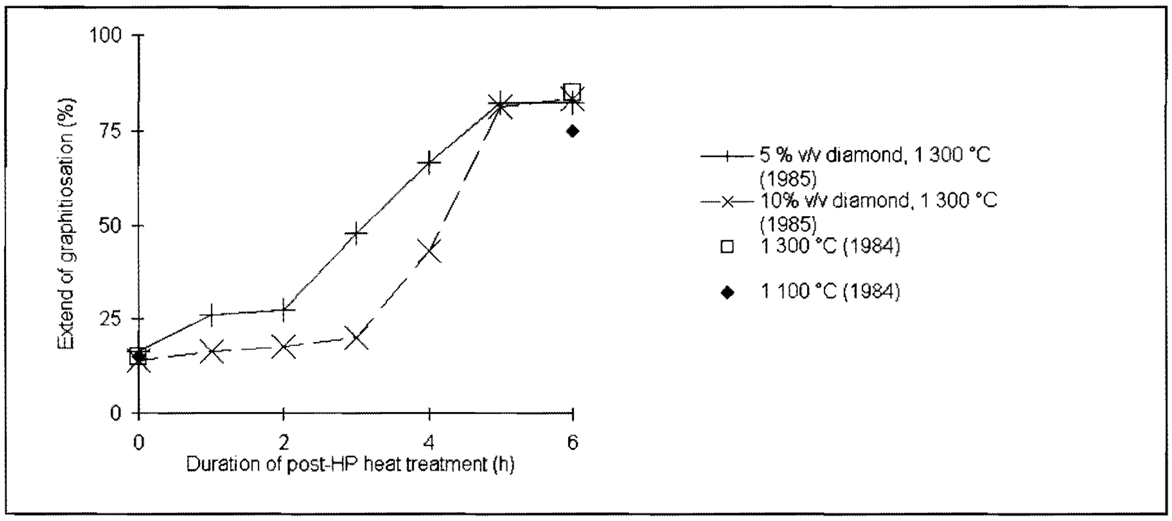

***Fig. 4-5**: Graphitisation of diamond in an alumina matrix after post densification heat (Noma and Sawaoka, 1984 and 1985).*

spectrum for diamond film deposited on alumina is shown. As such, it should not be directly comparable to the case of contact between non-deposited diamond and alumina as in the case of samples manufactured in this work. Nonetheless, one might intuitively expect similar peaking patterns.

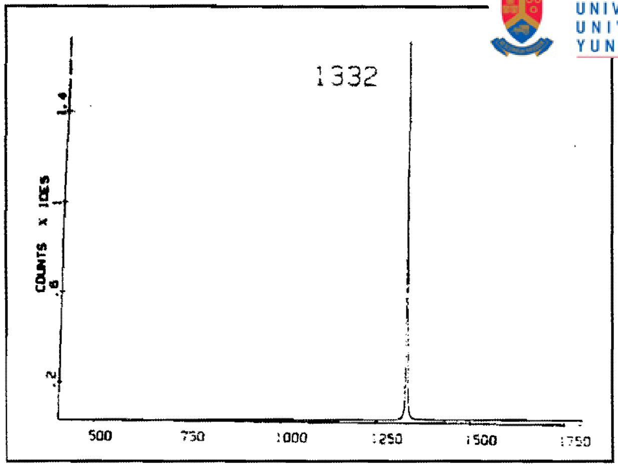

ctrum for natural diamond (Knight and White, 1989).

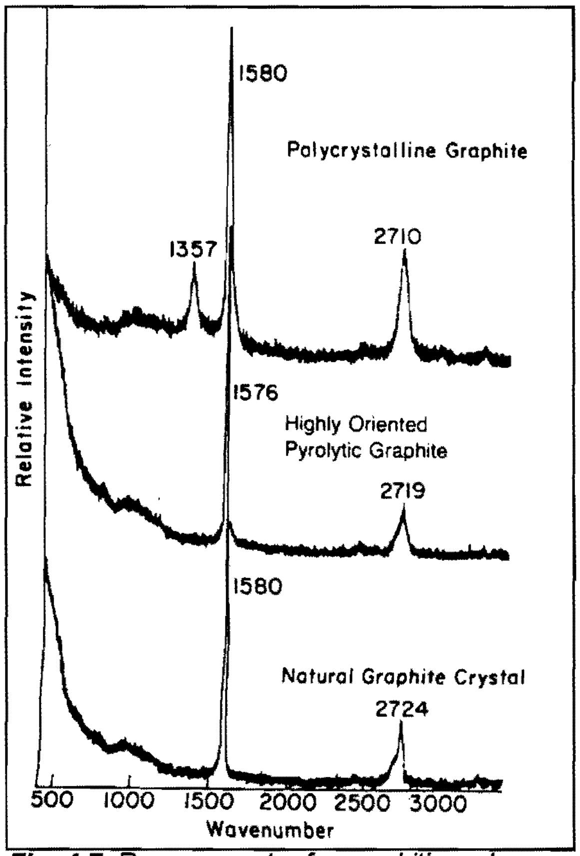

Fig. 4-7: *Raman spectra for graphitic carbon (Knight and White, 1989).*

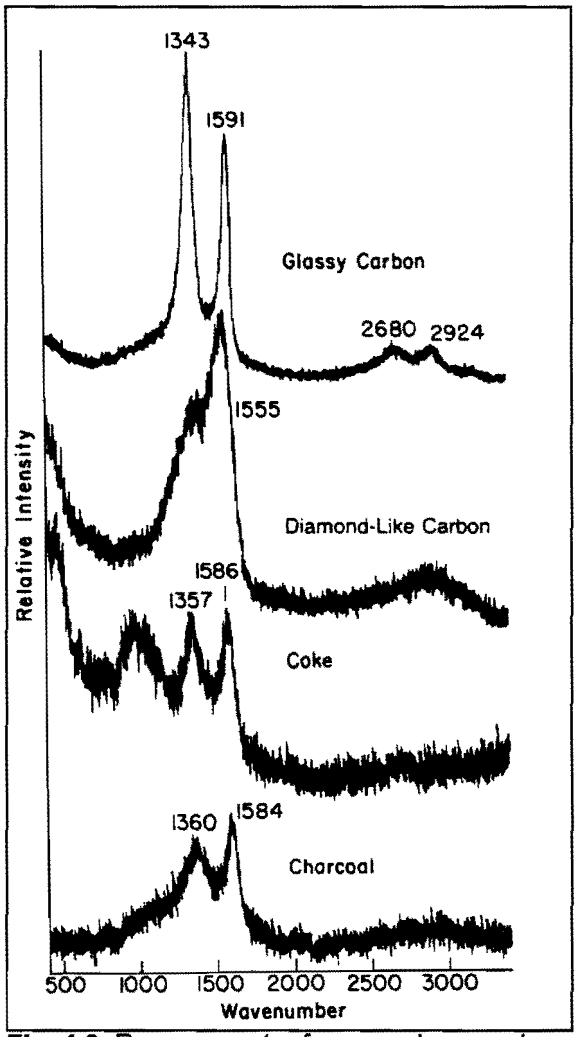

Fig. 4-8: *Raman spectra for amorphous carbon (Knight and White, 1989).*

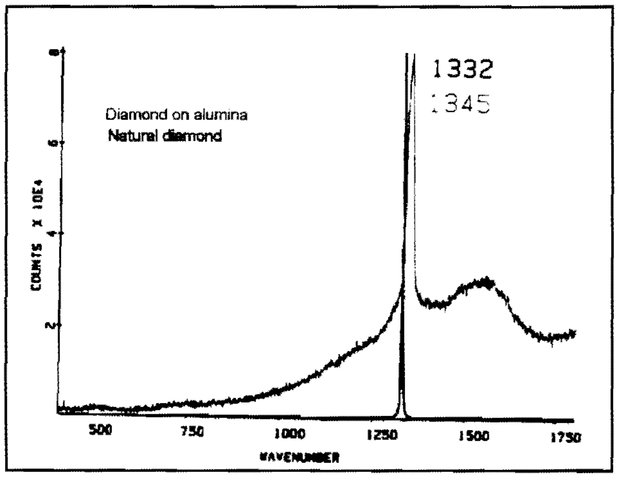

Fig. 4-9: *Raman spectra for diamond film deposited on alumina (Knight and White, 1989).*

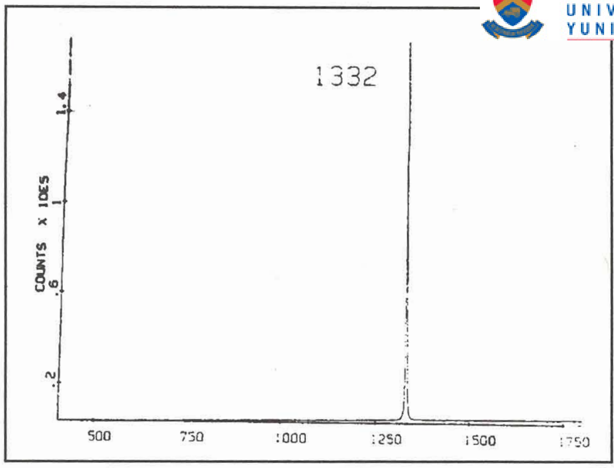

...ectrum for natural diamond (Knight and White, 1989).

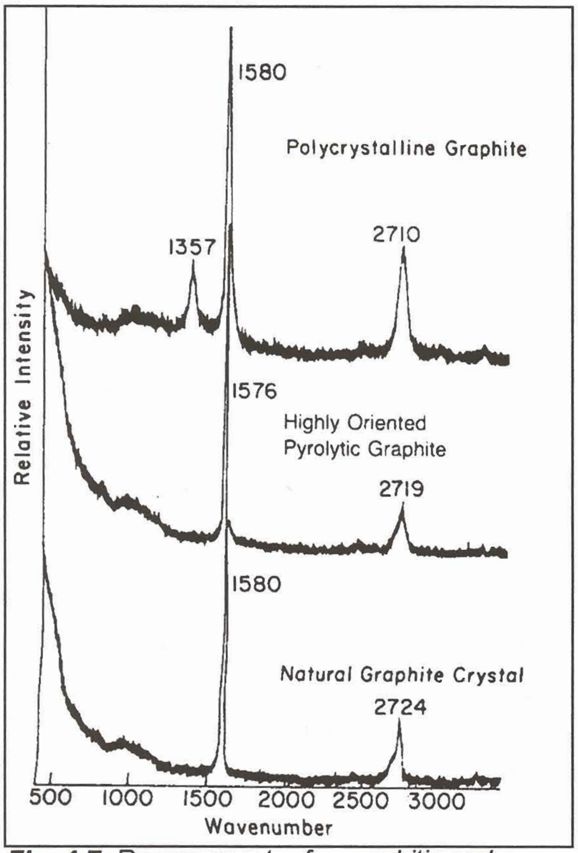

Fig. 4-7: *Raman spectra for graphitic carbon (Knight and White, 1989).*

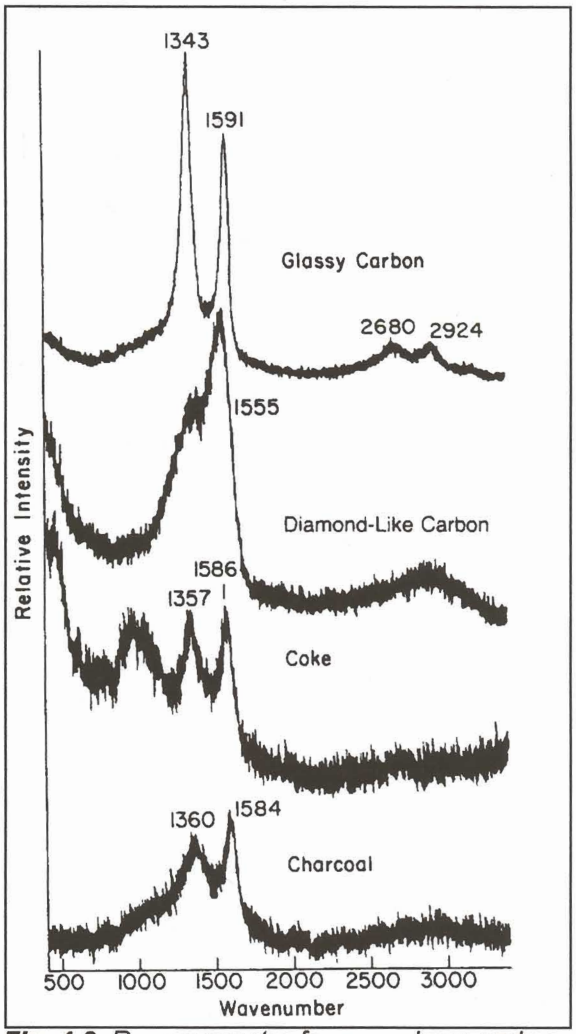

Fig. 4-8: *Raman spectra for amorphous carbon (Knight and White, 1989).*

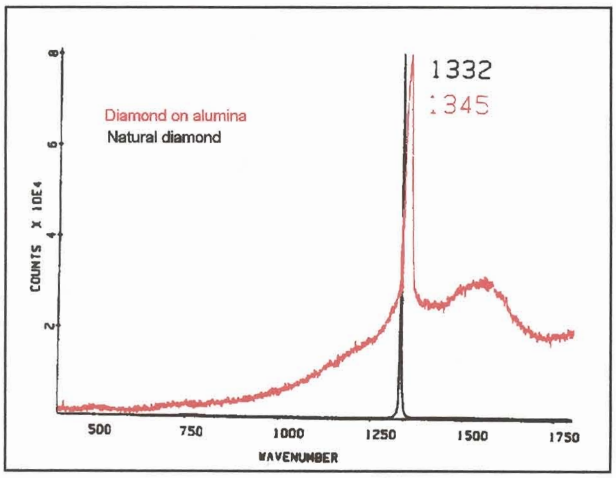

Fig. 4-9: *Raman spectra for diamond film deposited on alumina (Knight and White, 1989).*